

Discovering Motifs to Fingerprint Multi-Layer Networks: a Case Study on the Connectome of *C. Elegans*

Deepak Sharma^{1*}, Matthias Renz¹ and Philipp Hövel²

¹*Department of Computer Science, Christian-Albrechts Universität zu Kiel, Christian-Albrechts-Platz 4, Kiel, 24118, Germany.

²Theoretical Physics and Center for Biophysics, Saarland University, Campus E2 6, Saarbrücken, 66123, Germany.

*Corresponding author(s). E-mail(s): des@informatik.uni-kiel.de;
Contributing authors: mr@informatik.uni-kiel.de;
philipp.hoevel@uni-saarland.de;

Abstract

Motif discovery is a powerful approach to understanding network structures and their function. We present a comprehensive analysis of regulatory motifs in the connectome of the model organism *Caenorhabditis elegans* (*C. elegans*). Leveraging the Efficient Subgraph Counting Algorithmic PackagE (ESCAPE) algorithm, we identify network motifs in the multi-layer nervous system of *C. elegans* and link them to functional circuits. We further investigate motif enrichment within signal pathways and benchmark our findings with random networks of similar size and link density. Our findings provide valuable insights into the organization of the nerve net of this well documented organism and can be easily transferred to other species and disciplines alike.

Keywords: connectome analysis, network science, motif detection, *C. elegans*

1 Introduction

The nematode *Caenorhabditis elegans*, commonly known as *C. elegans*, has long been a prominent model organism in genetics and developmental biology research. Its relatively simple and well-defined anatomy, short life cycle, and fully sequenced genome

make it an ideal subject for investigating fundamental biological processes [1, 2]. Over the years, extensive studies on *C. elegans* have provided valuable insights into various aspects of cellular and molecular biology, contributing significantly to our understanding of eukaryotic biology [3–6].

In this study, we take a network-science driven angle [7] and focus on motif discovery in the nervous system of *C. elegans* to shed light on (i) the composition of the multi-layer connectome and (ii) the underlying regulatory circuits that govern the behavior of this model organism. The multi-layer nature arises from the presence of electrical (gap junction) and synaptic connections between the neurons. To achieve this, we adopt the *Efficient Subgraph Counting Algorithmic PackagE* (ESCAPE) algorithm [8], a powerful computational method that has proven effective in identifying regulatory motifs in complex data. We focus on network motifs that emerge from sets of 4 or 5 nodes and their connecting links such as triangles and cliques. Applying the ESCAPE algorithm to individual layers, the aggregaten network, and the locomotory circuit, we compare the distribution of these small-scale, recurrent network structures to random networks of similar size and link density. This allows identification of a fingerprint of the nervous system structure. We hypothesize that the ESCAPE algorithm will uncover novel and functionally relevant motifs in *C. elegans* that play crucial roles for the behaviors such as locomotion. By pursuing these objectives and testing our central hypothesis, we aim to provide valuable insights into the anatomical and functional landscape of the *C. elegans* connectome, exemplifying a universal approach to characterize network data in biology and beyond. This study holds the potential to advance our knowledge of networks in general and has implications in biological contexts in particular. Our approach is universally applicable and can be extended to network data (including directed links) of other sources and invites benchmarking against any network model.

The rest of the manuscript is organised as follows: In Section 2, we elaborate in the workflow and data set considered. Section 3 presents our findings and highlights exemplary cases of significant and insignificant motif occurrences. Finally, we conclude in Section 4.

2 Methods and Data

This section discusses the methodology applied for the motif discovery in the *C. elegans* data. We start with a summary of the multi-layer network and then, briefly review the ESCAPE framework [8].

2.1 Multi-Layer Network of *C. elegans*

The complexity of connectome structure in *C. elegans* extends beyond simple regulatory interactions, necessitating a comprehensive approach to capture the intricate relationships between anatomy and function. To achieve a more holistic understanding of the regulatory landscape, we consider a multi-layer network representation of *C. elegans*. This multi-layer network incorporates different layers of biological information, providing a powerful framework to investigate the interplay between neurons, connections, and their regulatory motifs. As discussed in the following, the multi-layer

structure consists of (i) electrical connections and (ii) synapses that involve different neurotransmitters, monoamines, and peptides (see Fig. 1 for the largest four layers in a circular layout):

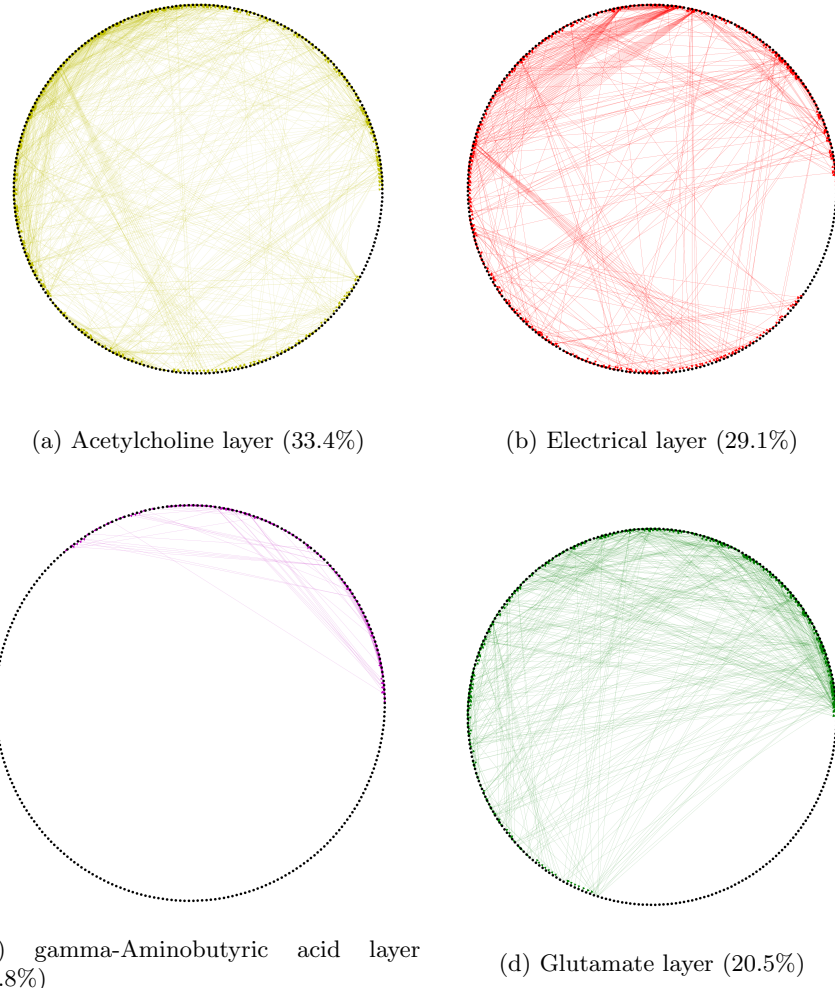


Fig. 1: The *C. elegans* multilayer network consists of nodes (circles) representing 279 neurons in a circular layout. In the aggregated network, there are 3,538 distinct connections among the nodes. Panels (a)-(d) show the links of 4 largest layers in terms of number of links: Acetylcholine (yellow), electrical (red), gamma-Aminobutyric acid (magenta), and Glutamate (green) layers, respectively.

Acetylcholine Layer (ACh): The Acetylcholine (ACh) layer, the largest component of the network, encompasses approximately 33.4% of the total 3,538 connections. It is distributed extensively across all neurons without showing a specific preference for any particular neuron type. In humans, ACh functions at skeletal neuromuscular junctions, interfaces between the vagus nerve and cardiac muscle fibers, as well as various locations within the central nervous system. Although ACh's role at neuromuscular junctions is well-documented, its precise function within the central nervous system remains a subject of incomplete understanding[9]. In the context of *C. elegans*, ACh is intricately involved in a multitude of behaviors, including but not limited to locomotion [10, 11], egg-laying [12], feeding [13], and defecation [14].

Electrical Layer: Electrical transmission, comprising 29.1% of network connections, is the second-largest layer after ACh. Electrical synapses are universally present in nervous systems, allowing direct bidirectional flow of electrical current between neurons. This mode of transmission is exceptionally fast, virtually instantaneous, enabling communication without delay, a departure from typical chemical synapses. Electrical synapses are located where rapid coordination and synchronization of network activity are required. For example, certain brainstem neurons synchronize via electrical synapses for rhythmic breathing, and similar synchronization occurs in interneuron populations in the cerebral cortex, thalamus, and cerebellum [9]. In *C. elegans*, electrical transmission plays a significant role in locomotion behavior and development [15, 16].

Gamma-Aminobutyric acid Layer (GABA): The gamma-Aminobutyric acid (GABA) layer stands as the smallest component within the network, accounting for approximately 3.8% of the connections. Most of these connections are established by interneurons and motor neurons. GABA serves as the neurotransmitter for approximately one third of the synapses in the brain and is predominantly found in interneurons within local circuits. Diverging from the excitatory nature of ACh and Glu, GABA exerts an inhibitory effect [9]. Notably, in *C. elegans*, GABA can also function as an excitatory transmitter, depending on the specific neuroreceptor involved. In its inhibitory role, GABA regulates head movements during foraging [17] and relaxes muscle cells during locomotion [18].

Glutamate Layer (Glu): The Glutamate (Glu) layer constitutes the third-largest component of the network, utilizing approximately 20.5% of its connections. In contrast to the ACh layer, this layer involves significantly fewer motor neurons. In the human brain, Glu plays a pivotal role as the primary neurotransmitter for normal brain function, with an estimated release from more than half of all brain synapses [9]. In the context of *C. elegans*, Glu contributes to various behavioral aspects, including foraging behavior [19], long-term memory processes [20], and spontaneous transitions from forward to backward movement, commonly referred to as reversals [21, 22].

Monoamine Layer (MA): MA transmitters constitute approximately 5.8% of network connections, with no specific neuron-type preference, although most motor neurons primarily receive postsynaptic signals. Among MA transmitters, dopamine accounts for about two-thirds. In humans, MAs play a crucial role in regulating various brain functions, extending from central homeostatic processes to cognitive phenomena like attention. Dysfunctions in MA function can lead to psychiatric disorders,

exemplified by Parkinson’s disease resulting from dopaminergic neuron degeneration [9]. In *C. elegans*, MAs influence a range of behaviors, including egg-laying, pharyngeal pumping, locomotion, and learning, as detailed in [1]. For instance, dopamine modulates locomotion behavior and learning, facilitating the worms’ responsiveness to environmental changes [23] and efficient exploration of new food sources [19]. Learning allows worms to adapt their behavior based on prior experiences, such as responding to non-localized mechanical stimuli like plate tapping by either moving backward or increasing forward locomotion, with repeated tapping leading to habituation and reduced reversal frequency [24].

Peptide Layer: Peptides account for approximately 11.8% of network connections, predominantly established by interneurons and sensory neurons, with most originating from the FLP and PDF families. Roughly 31% of these peptides act as neurotransmitters, while about 69% function as cotransmitters. In humans, peptides play roles in pain perception, emotional modulation, and complex responses to stress. Peptide cotransmission can modulate synaptic activity, impacting functions such as food intake, metabolism, social behavior, learning, and memory [9, 25]. In *C. elegans*, peptides influence a wide array of behaviors, including locomotion, dauer formation, egg-laying, sleep, learning, social behavior, mechano- and chemosensation. Notably, some FLP family peptides are involved in feeding behavior [26], while others, like nlp-22, regulate *C. elegans*’ sleep-like state (lethargus) during larval transitions[27]. Neuropeptides, constituting the third layer of information flow in neuronal communication alongside chemical and electrical transmission, are still not fully understood in *C. elegans*, with over 300 neuropeptides identified [28, 29]. Similar to monoamines, neuropeptides form a small wired network but a vast wireless network[30], suggesting their potential involvement in all *C. elegans* behaviors.

In the subsequent sections, we present our findings based on this multilayer network analysis, highlighting the discovery of regulatory motifs. This paves the way to understand their functional relevance, and the implications for understanding mechanisms governing *C. elegans* nervous system. We anticipate that the insights gained from this comprehensive multilayer network analysis will contribute significantly to the broader understanding of the *C. elegans* connectome and provide a valuable resource for the scientific community in further investigations that also invites the transfer of methodology to other model organisms and contexts.

2.2 Efficient Subgraph Counting Algorithmic PackagE: *ESCAPE*

In a nutshell, the applied algorithmic framework revolves around breaking down complex patterns into smaller sub-patterns and leveraging counts of these smaller patterns to obtain larger pattern counts. By employing this divide-and-conquer strategy, we can efficiently handle the enumeration and computation of subgraphs, even for large and complex networks. This approach allows us to avoid the excessive computational overhead associated with naively counting subgraphs. A key feature of the algorithm [8] is the exploitation of degree orientations within the graph. By judiciously utilizing

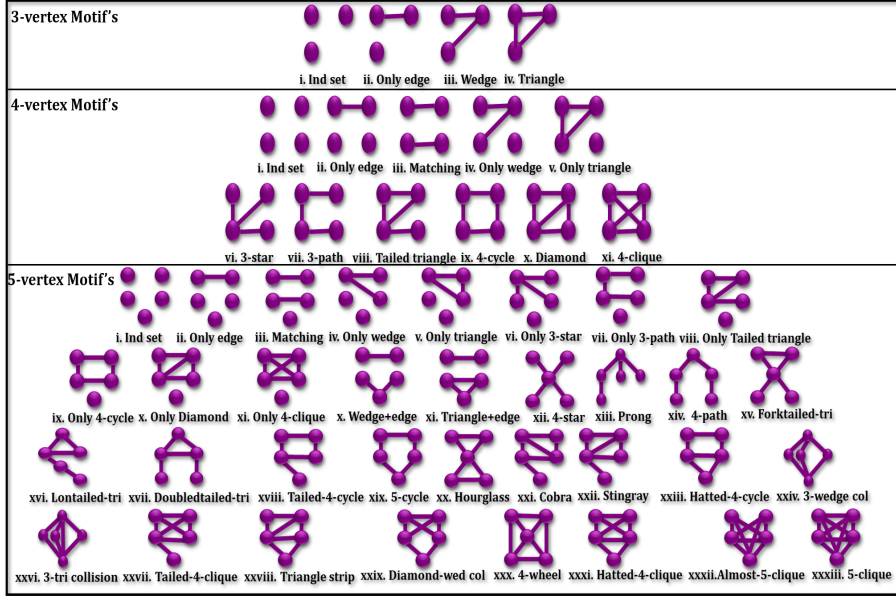


Fig. 2: Complete list 3-, 4- and 5-node motifs including names for later identification.

information about the degree distributions of vertices, we can further optimize runtime, resulting in faster computations. This optimization ensures that our algorithm can scale efficiently even for massive-sized graphs.

2.3 Motif Discovery Algorithm

The enumeration of graphlets, particularly in the context of large-scale graphs with millions of nodes and links, presents a formidable challenge due to the exponential growth in computational complexity. In the past, it was widely believed that subgraphs beyond three nodes were exceptionally difficult to enumerate, and conventional enumeration algorithms, which necessitate traversing each subgraph, were deemed impractical in terms of termination within a reasonable timeframe.

In response to the combinatorial explosion that hampers typical enumeration algorithms, the ESCAPE method was introduced by Pinar et al. [8]. This approach adopts a divide and conquer strategy, effectively identifying substructures within each counting subgraph and partitioning them into smaller patterns. Despite its broad applicability, the method allows for tailored decomposition choices that facilitate the derivation of a set of formulas to compute the frequency of each subgraph efficiently. While the original paper delineates the resulting formulas for subgraphs up to size 5, diligent efforts can extend the application to larger sizes.

To the best of our knowledge, ESCAPE stands as one of the most efficient algorithms available for counting undirected subgraphs and orbits up to size 5. Its strength lies in the ability to mitigate the exponential growth in complexity, enabling the enumeration of graphlets even in sizable graphs with millions of vertices and links.

Through its divide-and-conquer paradigm and strategic substructure identification, ESCAPE opens new avenues for motif discovery, offering unprecedented opportunities to unravel recurring patterns within complex networks. Its scalability and performance make it a compelling choice for motif analysis in diverse domains, such as social networks, biological networks, and recommendation systems.

2.4 Proposed Methodology

Next, we describe the stepwise methodology of the proposed work for *C. elegans* motif discovery. As schematically depicted in Fig. 3, the pipeline includes the following steps:

- Step 1:** Input: Reading multilayer network data and generation of random networks of the same size
- Step 2:** Analysis: Application of the ESCAPE algorithm
- Step 3:** Output: Motif distribution
- Step 3:** Comparison: Benchmarking empirical against random networks
- Step 4:** Comparison: Identification of significant motifs

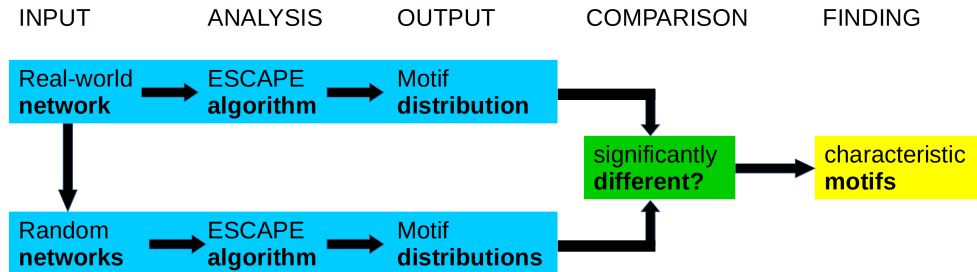


Fig. 3: Pipeline for the motif discovery.

The selection of random networks is one of many choices of network classes to generate artificial networks for benchmarking. Other prominent examples include regular, small-world, or scale-free networks, to name but a few. For the proper determination of a motif's sub-network significance, we need comparison by an ensemble of a reference network class, e.g. random graphs. Thus, the generation of this ensemble due to a given random graph model is a necessary step of the algorithm. One of the popular random graph models on which we also focused is to preserve the degree sequence of the original graph in random graphs. Note there has been some research concerning the problem of sub-graph distribution within such graphs for directed sparse random graphs [31, 32].

We follow a randomizing approach to generate reference networks of the same number of nodes and links. In that approach, similar to Milo's random model [31, 32], switching operations are repeatedly applied on the randomly chosen vertices of the input network and their links, until the network is well randomized. By applying these switching operations, an ensemble of random networks is generated for comparing the real network to obtain the significance of each motif.

For the significance of occurrence of each motif, statistical measures are introduced that lead us to the probable motifs in the input network: (i) *Frequency*: This is the simplest measurement for estimating the significance of a motif. The frequency is defined as the number of occurrences of a motif P in the network. (ii) KS test: We employ the Kolmogorov-Smirnov (KS) test to identify significant and insignificant motif frequencies by comparing the input network's motif frequency with those from 1000 generated random networks. First, the motif P frequency is counted in the input network. Then, the same motif is counted in each of the random networks, creating a distribution of motif frequencies for comparison. (iii) *p-value*: The KS test compares the motif frequency distribution of the input network against the random networks' distributions, providing a p-value to indicate significance. A low p-value signifies that the motif frequency is significantly different from random, indicating the motif's significance, while a high p-value indicates insignificance. Therefore, p-values range from 0 to 1. The smaller the p-value, the more significant the motif. Here, we consider a p-value of 0.05, below which we declare the occurrence of a motif as significant, that is, characteristic.

3 Results and Performance Evaluation

This section provides the details of dataset and performance indicators used for the experiment analysis.

Table 1: Data description: Number of nodes and links for the different layers, the aggregated network (All), and the locomotory circuit (LC).

	ACh	Electrical	GABA	Glu	MA	Peptides	All	LC
Nodes	258	253	102	197	131	162	279	83
Links	1145	1028	133	727	212	455	3700	435
Undirected links	1080	514	130	708	203	401	2287	435

3.1 Data

The dataset [33] used in this study encompasses a comprehensive network representation of a biological system, capturing the interactions between various types of molecular entities. The data consists of nodes and links, representing different neuronal units and their connections within the biological system. The dataset contains a total of 279 nodes and 3,538 links. These nodes refer to neurons, each contributing to the overall functionality of the nervous system. The links in the network represent the connections or interactions between the neurons. A total of 3,538 links have been identified in the dataset across several layers (cf. Fig. 1), signifying the complex web of interactions within the biological system. Table 1 provides an overview of the data, showcasing the different layers and the number of neurons involved as nodes in the network and the number of links that connect them. Each network layer corresponds to a specific neurotransmitter or signaling molecule involved in the biological system

under investigation. The last two columns represent the total number of nodes in the aggregated network and the locomotory circuit, which is added as a functionally relevant subnetwork. In total, there are 3700 aggregated links, which amounts to 3,538 distinct connections between the neurons. Note that the electrical layer is – for reasons of neuro-physiology – bi-directional. All other layers are uni-directional. For the purpose of this study, we ignore the directionality and treat the connection as undirected. The last row of Table 1 shows the number of links in the considered undirected network.

3.2 Network motifs

Next, we present the results of our analysis on the multi-layer network of *C. elegans* using the ESCAPE algorithm [8] for counting small sub-network patterns. Specifically, we focus on motifs consisting of 3, 4, and 5 nodes and their prevalence across the different layers within the network. Additionally, we discuss the findings and implications of our motif counting analysis.

3.2.1 3-node motifs

Table 2 summarizes the number of occurrence of all possible motifs involving 3 nodes, from the independent set (3 nodes with no links) to the triangle (3-clique or all-to-all connected set of 3 nodes). Obviously, the former is given by the binomial coefficient $\binom{N}{3}$, where N denotes the number of nodes in the layer (cf. Tabl 1). Evaluating the occurrences, it is important to note that a brute-force calculation of the motifs inevitably leads to double and multiple countings. For instance, a triangle automatically includes 3 motifs of wedge type. Here, network science/graph theory comes to our aid and provides the notion of non-induced and induced sub-networks.

Table 2: 3-node non-induced motif in *C. elegans* multi-layer network

	Motif	ACh	Electrical	GABA	Glu	MA	Peptides	All	LC
Ind set		2829056	2667126	171700	1254890	366145	695520	3580779	91881
Only link		276480	129014	13000	138060	26187	64160	633499	35235
wedge		16848	3972	678	8035	1565	3028	56984	7056
Triangle		1083	170	18	376	28	125	4055	680

As illustrated in Fig. 4, a *non-induced* sub-network consists of a set of nodes, but not all possible edges that are present in the original network. In contrast, a motif is called *induced* if it contains the maximum set of links connecting its nodes in the

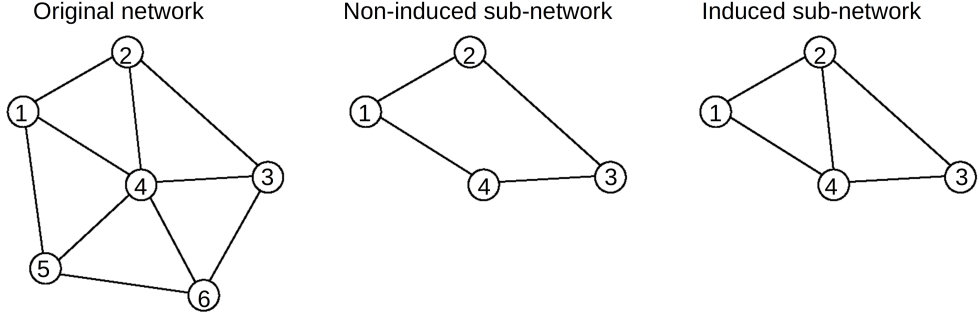


Fig. 4: Schematics of a 6-node network, a non-induced 4-node sub-networks, and an induced 4-node sub-networks. The latter consists of the maximum number of nodes and links taken from the original network.

original network. In the schematic example, the link between nodes 2 and 4 is missing in the non-induced sub-network of nodes 1, 2, 3, and 4, while it is accounted for in the induced one. One can convert from the induced to the non-induced count by multiplying with a transformation matrix that provides the combinatorics of lower-motif inclusions. For 3- and 4-node motifs, it is given by

$$A_3 = \begin{pmatrix} 1 & 1 & 1 & 1 \\ 0 & 1 & 2 & 2 \\ 0 & 0 & 1 & 3 \\ 0 & 0 & 0 & 1 \end{pmatrix}, \quad A_4 = \begin{pmatrix} 1 & 1 & 1 & 1 & 1 & 1 & 1 & 1 & 1 & 1 \\ 0 & 1 & 2 & 2 & 3 & 3 & 3 & 4 & 4 & 5 & 6 \\ 0 & 0 & 1 & 0 & 0 & 0 & 1 & 1 & 2 & 2 & 3 \\ 0 & 0 & 0 & 1 & 3 & 3 & 2 & 5 & 4 & 8 & 12 \\ 0 & 0 & 0 & 0 & 1 & 0 & 0 & 1 & 0 & 2 & 4 \\ 0 & 0 & 0 & 0 & 0 & 1 & 0 & 1 & 0 & 2 & 4 \\ 0 & 0 & 0 & 0 & 0 & 0 & 1 & 2 & 4 & 6 & 12 \\ 0 & 0 & 0 & 0 & 0 & 0 & 0 & 1 & 0 & 4 & 12 \\ 0 & 0 & 0 & 0 & 0 & 0 & 0 & 0 & 1 & 1 & 3 \\ 0 & 0 & 0 & 0 & 0 & 0 & 0 & 0 & 0 & 1 & 6 \\ 0 & 0 & 0 & 0 & 0 & 0 & 0 & 0 & 0 & 0 & 1 \end{pmatrix}, \quad (1)$$

where the ordering of motifs corresponds to Fig. 2. See Appendix of Ref. [8] for the 33×33 transformation matrix A_5 of 5-node motifs.

Therefore, it is helpful to focus on the occurrences of induced motifs, which is given in Tab. 3. That way, the count reflects sub-networks that are not part of a motif with the same set of nodes connected with more links. One can quantify the different via the ratio of induced to non-induced motifs. As shown in Tab. 4 that ratio is rather high, that is close to unity. For instance, considering the ACh layer, we find that 13599 wedges do not stem from triangles with one link left out. In fact, one can easily verify that the difference between the number of wedges of the induced to the non-induced case equals 3 times the number of triangles. In the following, we will consider only induced motifs. The tables for the non-induced case for both the original and reference networks can be found in Appendices A–F.

Table 3: 3-node induced motif in *C. elegans* multi-layer network

Motif	Motif	ACh	Electrical	GABA	Glu	MA	Peptides	All	LC
Ind set		2568341	2541914	159360	1124489	341495	634263	3000209	63022
Only link		246033	121580	11698	123118	23141	58479	531696	23163
wedge		13599	3462	624	6907	1481	2653	44819	5016
Triangle		1083	170	18	376	28	125	4055	680

Table 4: Ratio of 3-node induced vs non-induced motif in *C. elegans* multi-layer network

	Motif	ACh	Electrical	GABA	Glu	MA	Peptides	All	LC
Ind set		0.91	0.95	0.93	0.9	0.93	0.91	0.84	0.69
Only link		0.89	0.94	0.9	0.89	0.88	0.91	0.84	0.66
wedge		0.81	0.87	0.92	0.86	0.95	0.88	0.79	0.71
Triangle		1.00	1.00	1.00	1.00	1.00	1.00	1.00	1.00

3.2.2 4-node motifs

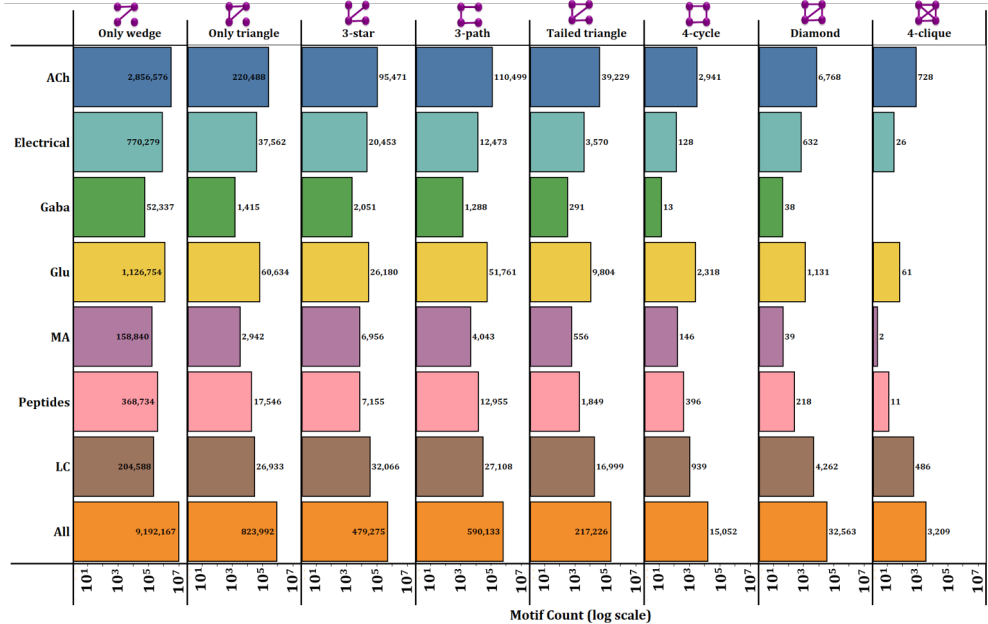


Fig. 5: Histogram of induced 4-node motifs in each layer. See Tab. 5 for a comparison to the non-induced counts given in Tab. A1.

Figure 5 showcases the histogram of the counts of various 4-node motifs identified within the multi-layer network, classified by different molecular entity types, including ACh, Electrical, GABA, Glu, Monoamines, Peptides, and All (representing the total, aggregated network). Each motif type is represented by a corresponding graphical depiction. Note that the result of the independent set, only edge, and mathtt{m}ing motifs are not shown. The respective numbers can be found in Appendix C.

To highlight some numbers: The motif representing a wedge-plus-independent-node configuration (an unconnected pair of nodes sharing a common neighbor) is prevalent across all molecular entity types, with counts ranging from 2856576 in the ACh layer to 52337 in the GABA layer. In the aggregated network, we observe a total count of more than 9 million wedge motifs. Triangles (three nodes interconnected in a closed loop plus a single independent node) are also frequently observed across the network, with counts varying from 220488 in the ACh layer to 1415 in the GABA layer, with a total count of 823992 in the combined-layer network.

As the motif structure becomes more elaborate, the number of occurrences decreases. The diamond (two pairs of nodes connected by a central node) and 4-clique (four fully interconnected nodes) motifs feature the least among all 4-node motifs. In fact, there is not a single occurrence of a 4-clique in the GABA layer.

Table 5: Ratios of 4-node induced vs non-induced motif in *C. elegans* multi-layer network. The values in bold indicate that the discovered induced motif count is not significant.

	Motif	ACh	Electrical	GABA	Glu	MA	Peptides	All	LC
Ind set		0.83	0.91	0.86	0.81	0.87	0.83	0.71	0.50
Only link		0.77	0.88	0.79	0.77	0.77	0.81	0.67	0.41
Matching		0.70	0.86	0.78	0.72	0.74	0.79	0.64	0.36
Only wedge		0.66	0.78	0.78	0.72	0.79	0.77	0.58	0.36
Only triangle		0.80	0.88	0.79	0.83	0.82	0.88	0.74	0.50
3-star		0.63	0.81	0.85	0.68	0.92	0.75	0.62	0.54
3-path		0.44	0.51	0.60	0.59	0.67	0.66	0.45	0.28
Tailed triangle		0.52	0.56	0.66	0.65	0.76	0.65	0.56	0.43
4-cycle		0.25	0.15	0.25	0.64	0.76	0.61	0.26	0.14
Diamond		0.61	0.80	1.00	0.76	0.76	0.77	0.63	0.59
4-clique		1.00	1.00	-	1.00	1.00	1.00	1.00	1.00

The ratios of the induced and non-induced 4-node motifs are given in Table 4 (See Appendix A for the absolute values of the non-induced motifs). We find that for sparser layers such as Glu and MA motifs with more links do not tend to be part of higher-order motifs, that is, they are induced. See, for instance, ratios of 0.92 (0.63) or 0.76 (0.25) for 3-start and 4-cycle motifs in the MA (ACh) layer.

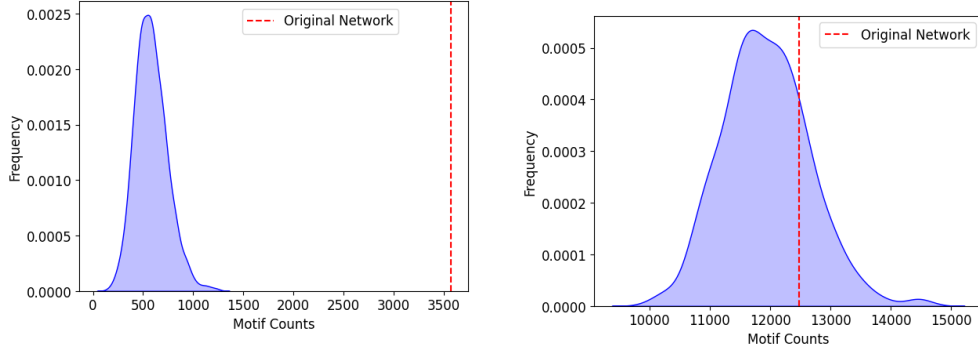
The results of the occurrences of motifs in each layered compared to the aggregated network are summarized in Tab. A2. Here, one can see the difference between edges formed by electrical gap junctions and chemical synapses. Although the electrical layer form the second-largest layer, in terms of both number of nodes and edges, its contribution to the motif count is rather small. In other works, most of the motifs are found in the chemical layers. Furthermore, the ACh layer, while represented at almost 50% of the connections in the aggregated network (cf. Tab.1) do not feature

Table 6: Percentage of 4-node induced motif in *C. elegans* multi-layer network relative to ALL (aggregated network). The values in bold indicate that the discovered motif count is not significant.

	Motif	ACh	Electrical	GABA	Glu	MA	Peptides
Ind set		85.29	86.57	2.1	28.03	5.85	13.17
Only link		46.24	23.98	0.87	17.51	2.18	6.98
Matching		23.98	6.7	0.37	10.55	0.85	3.72
Only wedge		31.08	8.38	0.57	12.26	1.73	4.01
Only triangle		26.76	4.56	0.17	7.36	0.36	2.13
3-star		19.92	4.27	0.43	5.46	1.45	1.49
3-path		18.72	2.11	0.22	8.77	0.69	2.20
Tailed triangle		18.06	1.64	0.13	4.51	0.26	0.85
4-cycle		19.54	0.85	0.09	15.4	0.97	2.63
Diamond		20.78	1.94	0.12	3.47	0.12	0.67
4-clique		22.69	0.81	0.00	1.9	0.06	0.34

that prominently in the motif count. This means that many chemical links involve more than just a single neurotransmitter.

In order to identify the occurrences of significant motifs, we compare the motif distributions of the original network to 1000 random networks with the same number of nodes and edges and repeat the motif analysis. The resulting average counts of the different induced and non-induced 4-node motifs are given in Appendices B and D, respectively. As an exemplary illustration, Fig. 6 depicts the case of a significant motif (tailed triangle) in panel (a) and an insignificant motif (3-path) in panel (b). One can clearly see that the number of tailed-triangle motifs (3570) lies outside the distribution calculated for the random networks, while the the number of 3-path motifs (12473) can also be found in a substantial amount of random reference networks. Interestingly, we find only a few cases of insignificant induced motifs. These are indicated by bold values



(a) Significance of tailed-triangle motif in the electrical layer as shown in Fig. 5 and Table C5.

(b) Insignificance of 3-path motif in electrical layer as shown in Fig. 5 and Table C5.

Fig. 6: Examples for a significant and an insignificant 4-node induced motif in the electrical layer of original network (cf. Fig. 5) as compared to the random reference networks.

in Tabs. 6, 5, and C5. Moreover, in almost all cases of significant motifs, the counts extracted from the original network is far away from those of the random reference networks.

3.2.3 5-node motifs

Next, we turn our attention to motifs that involve 3 nodes, and focus on those subnetwork structures that cannot be part of a 4-node motif with 1 additional unconnected node. This includes 23 out of 33 possible 5-node motifs (cf. Fig. 2).

Table 3.2.3 summarizes the findings in terms of the percentage of 5-node induced motif relative the aggregated network case. Again, we find that almost all motifs are significant in their occurrence and cannot be expected from random reference networks. It is noteworthy that the overwhelming majority of insignificant motif counts (except the wedge+link motif) appear for very small fractions below 1 percent. In those cases, their existence is unlikely in random networks as well. The absolute values and numbers for non-induced 5-node motifs can be found in Appendices E to H for the sake of completeness, but are not displayed here to improve readability.

Table 7: Percentage of 5-node induced motif in *C. elegans* multi-layer network relative to ALL (aggregated network). The values in bold indicate that the discovered motif count is not significant.

	Motif	ACh	Electrical	GABA	Glu	MA	Peptides
wedge+link		16.15	2.67	0.10	5.80	0.35	1.49
Triangle+link		13.08	1.43	0.03	3.33	0.08	0.78
4-star		12.38	2.33	0.1	1.41	0.50	0.28
Prong		12.55	1.01	0.08	3.60	0.31	0.66
4-path		11.41	0.80	0.04	5.33	0.21	0.93
Forktailed-tri		11.25	0.91	0.04	1.42	0.11	0.16
Lontailed-tri		10.15	0.48	0.02	2.86	0.05	0.39
Doubletailed-tri		12.77	0.46	0.04	2.51	0.12	0.27
Tailed-4-cycle		11.72	0.4	0.02	6.95	0.35	0.82
5-cycle		8.76	0.33	0.01	4.11	0.14	0.63
Hourglass		7.30	0.31	0.01	1.58	0.02	0.15

Table 7: Percentage of 5-node induced motif in *C. elegans* multi-layer network relative to ALL (aggregated network). The values in bold indicate that the discovered motif count is not significant.

Cobra		13.39	0.41	0.02	2.22	0.01	0.24
Stingray		13.56	0.80	0.03	1.29	0.06	0.12
Hatted-4-cycle		9.55	0.16	0.01	3.72	0.08	0.39
3-wedge-col		18.5	0.16	0.02	20.50	0.97	1.40
3-tri-collison		15.83	1.96	0.04	0.72	0.02	0.09
Tailed-4-clique		15.66	0.28	0.00	0.95	0.00	0.07
Triangle-strip		12.06	0.31	0.01	1.31	0.00	0.13
Diamond-wed-col		13.78	0.15	0.01	5.88	0.04	0.51
4-Wheel		16.19	0.21	0.01	3.11	0.00	0.22
Hatted-4-clique		15.89	0.46	0.00	0.56	0.00	0.08
Almost-5-clique		19.34	0.13	0.00	0.45	0.01	0.01
5-clique		23.11	0.00	0.00	0.06	0.00	0.00

The exact numbers are also included in Fig. 7 in addition to the histograms. We find that in general, more complex motifs are present on lower numbers and are completely absent on small layers. At the same time, layers with more nodes and links have the tendency to allow for these motifs, e.g., 4-wheel, hatted-4-clique, almost-5-clique, or 5-clique (see bottom panel of Fig. 7), and the corresponding motifs remain significant to characterize the layer.

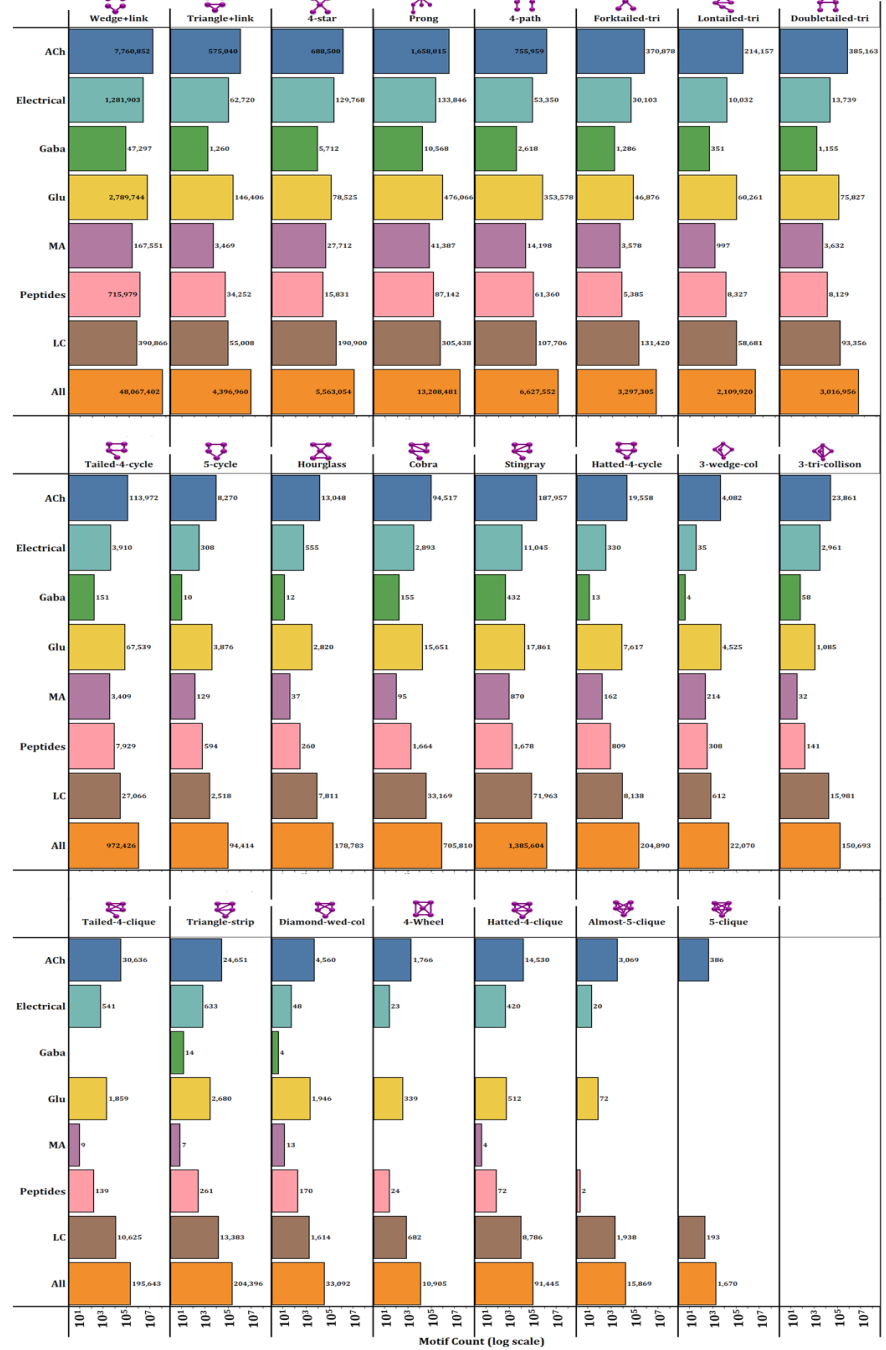


Fig. 7: Histogram of induced 5-node motif in each layer. See Tab. G for a comparison to the non-induced counts given in Tab. E.

4 Conclusions

We have presented the application of a motif-discovery algorithm for network analysis. As a case study, the algorithm has been applied to the multi-layer connectome of *C. elegans*. We have considered motifs formed by 3, 4, or 5 nodes. Our analysis of the motif occurrences has yielded several important findings. First, the abundance of wedge motifs indicates the prevalence of shared regulators across different layers corresponding to different molecular entities (neurotransmitters), reflecting the existence of conserved regulatory mechanisms. Additionally, the presence of motifs with closed paths such as triangles, 4- or 5-cycles and their various variants with extensions to the core cycle suggests the occurrence of regulatory feedback. Similarly, stars of spokes-and-hub shape point to central regulators in the network.

To identify significant motifs, we have compared the original network to an ensemble of 1000 random networks of the same number of nodes and links. For almost all layers and motif types, we find that the occurrence of motifs cannot be explained by a random network model. Notably, the 3-path and 4-path motifs stand out as an exception of insignificant motifs in the electrical and GABA layer, which are not suited to characterize the network at hand. Interestingly, the presence of 4-cycles and diamonds across multiple layers implies recurrent regulatory patterns and interconnected information pathways. Conversely, 4- and 5-clique motifs feature less prominently which suggests that fully interconnected regulatory clusters are less prevalent in the network.

The proposed approach can be easily extended in several directions: (i) It invites the characterization of significant and insignificant motifs in other empirical networks from various background. (ii) We have chosen random networks as reference case. The pipeline, however, allows to consider other classes of networks as well. That way, a network extracted from an empirical dataset can be fingerprinted and uniquely characterized by its composition of small network substructures.

Acknowledgment

We are grateful to Karlheinz Ochs, Sebastian Jenderny, and Christian Beth for stimulating discussions. This work was funded by the Deutsche Forschungsgemeinschaft (DFG—German Research Foundation) under Project ID: 434434223-SFB 1461.

References

- [1] Chase, D.L., Koelle, M.R.: Biogenic amine neurotransmitters in *C. elegans*. WormBook: The Online Review of *C. elegans* Biology [Internet] (2007)
- [2] Yan, G., Vértes, P.E., Towlson, E.K., Chew, Y.L., Walker, D.S., Schafer, W.R., Barabási, A.-L.: Network control principles predict neuron function in the *Caenorhabditis elegans* connectome. *Nature* **550**(7677), 519–523 (2017)
- [3] Towlson, E.K., Vértes, P.E., Ahnert, S.E., Schafer, W.R., Bullmore, E.T.: The rich club of the *C. elegans* neuronal connectome. *Journal of Neuroscience* **33**(15), 6380–6387 (2013)
- [4] Dag, U., Nwabudike, I., Kang, D., Gomes, M.A., Kim, J., Atanas, A.A., Bueno, E., Estrem, C., Pugliese, S., Wang, Z., *et al.*: Dissecting the functional organization of

- the *C. elegans* serotonergic system at whole-brain scale. *Cell* **186**(12), 2574–2592 (2023)
- [5] Towlson, E.K., Barabási, A.-L.: Synthetic ablations in the *c. elegans* nervous system. *Network Neuroscience* **4**(1), 200–216 (2020)
 - [6] Chew, Y.L., Walker, D.S., Towlson, E.K., Vértes, P.E., Yan, G., Barabási, A.-L., Schafer, W.R.: Recordings of *Caenorhabditis elegans* locomotor behaviour following targeted ablation of single motoneurons. *Scientific Data* **4**(1), 1–7 (2017)
 - [7] Barabási, D.L., Bianconi, G., Bullmore, E., Burgess, M., Chung, S., Eliassi-Rad, T., George, D., Kovács, I.A., Makse, H., Nichols, T.E., *et al.*: Neuroscience needs network science. *Journal of Neuroscience* **43**(34), 5989–5995 (2023)
 - [8] Pinar, A., Seshadhri, C., Vishal, V.: Escape: Efficiently counting all 5-vertex subgraphs. In: Proceedings of the 26th International Conference on World Wide Web, pp. 1431–1440 (2017)
 - [9] Purves, D., Augustine, G.J., Fitzpatrick, D., Hall, W., LaMantia, A.-S., White, L.: Neurosciences. De Boeck Supérieur, ??? (2019)
 - [10] Winnier, A.R., Meir, J.Y.-J., Ross, J.M., Tavernarakis, N., Driscoll, M., Ishihara, T., Katsura, I., Miller, D.M.: UNC-4/UNC-37-dependent repression of motor neuron-specific genes controls synaptic choice in *Caenorhabditis elegans*. *Genes & development* **13**(21), 2774–2786 (1999)
 - [11] Hallam, S., Singer, E., Waring, D., Jin, Y.: The *C. elegans* NeuroD homolog cnd-1 functions in multiple aspects of motor neuron fate specification. *Development* **127**(19), 4293–4301 (2000)
 - [12] Bany, I.A., Dong, M.-Q., Koelle, M.R.: Genetic and cellular basis for acetylcholine inhibition of *Caenorhabditis elegans* egg-laying behavior. *Journal of Neuroscience* **23**(22), 8060–8069 (2003)
 - [13] Raizen, D.M., Lee, R., Avery, L.: Interacting genes required for pharyngeal excitation by motor neuron MC in *Caenorhabditis elegans*. *Genetics* **141**(4), 1365–1382 (1995)
 - [14] Thomas, J.H.: Genetic analysis of defecation in *Caenorhabditis elegans*. *Genetics* **124**(4), 855–872 (1990)
 - [15] Hall, D.H.: Gap junctions in *C. elegans*: Their roles in behavior and development. *Developmental neurobiology* **77**(5), 587–596 (2017)
 - [16] Simonsen, K.T., Moerman, D.G., Naus, C.C.: Gap junctions in *C. elegans*. *Frontiers in physiology* **5**, 40 (2014)

- [17] White, J.G., Southgate, E., Thomson, J.N., Brenner, S., *et al.*: The structure of the nervous system of the nematode *Caenorhabditis elegans*. *Philos Trans R Soc Lond B Biol Sci* **314**(1165), 1–340 (1986)
- [18] McIntire, S.L., Jorgensen, E., Horvitz, H.R.: Genes required for GABA function in *Caenorhabditis elegans*. *Nature* **364**(6435), 334–337 (1993)
- [19] Hills, T., Brockie, P.J., Maricq, A.V.: Dopamine and glutamate control area-restricted search behavior in *caenorhabditis elegans*. *Journal of Neuroscience* **24**(5), 1217–1225 (2004)
- [20] Rose, J.K., Kaun, K.R., Chen, S.H., Rankin, C.H.: GLR-1, a non-NMDA glutamate receptor homolog, is critical for long-term memory in *Caenorhabditis elegans*. *Journal of Neuroscience* **23**(29), 9595–9599 (2003)
- [21] Zheng, Y., Brockie, P.J., Mellem, J.E., Madsen, D.M., Maricq, A.V.: Neuronal control of locomotion in *C. elegans* is modified by a dominant mutation in the GLR-1 ionotropic glutamate receptor. *Neuron* **24**(2), 347–361 (1999)
- [22] Brockie, P.J., Mellem, J.E., Hills, T., Madsen, D.M., Maricq, A.V.: The *C. elegans* glutamate receptor subunit NMR-1 is required for slow NMDA-activated currents that regulate reversal frequency during locomotion. *Neuron* **31**(4), 617–630 (2001)
- [23] Sawin, E.R., Ranganathan, R., Horvitz, H.R.: *C. elegans* locomotory rate is modulated by the environment through a dopaminergic pathway and by experience through a serotonergic pathway. *Neuron* **26**(3), 619–631 (2000)
- [24] Rose, J.K., Rankin, C.H.: Analyses of habituation in *Caenorhabditis elegans*. *Learning & Memory* **8**(2), 63–69 (2001)
- [25] Russo, A.F.: Overview of neuropeptides: Awakening the senses? *Headache: The Journal of Head and Face Pain* **57**, 37–46 (2017)
- [26] Li, C., Kim, K.: Neuropeptides. *WormBook: The Online Review of *C. elegans* Biology*. WormBook (2018)
- [27] Nelson, M., Trojanowski, N., George-Raizen, J., Smith, C., Yu, C.-C., Fang-Yen, C., Raizen, D.: The neuropeptide NLP-22 regulates a sleep-like state in *Caenorhabditis elegans*. *Nature communications* **4**(1), 2846 (2013)
- [28] Ringstad, N.: Neuromodulation: The fevered mind of the worm. *Current Biology* **27**(8), 315–317 (2017)
- [29] Chew, Y.L., Grundy, L.J., Brown, A.E., Beets, I., Schafer, W.R.: Neuropeptides encoded by *nlp-49* modulate locomotion, arousal and egg-laying behaviours in *Caenorhabditis elegans* via the receptor SEB-3. *Philosophical Transactions of the*

Royal Society B: Biological Sciences **373**(1758), 20170368 (2018)

- [30] Bentley, B., Branicky, R., Barnes, C.L., Chew, Y.L., Yemini, E., Bullmore, E.T., Vértes, P.E., Schafer, W.R.: The multilayer connectome of *Caenorhabditis elegans*. PLoS computational biology **12**(12), 1005283 (2016)
- [31] Maslov, S., Sneppen, K.: Specificity and stability in topology of protein networks. Science **296**(5569), 910–913 (2002)
- [32] Milo, R., Kashtan, N., Itzkovitz, S., Newman, M.E., Alon, U.: On the uniform generation of random graphs with prescribed degree sequences. arXiv preprint cond-mat/0312028 (2003)
- [33] Maertens, T., Schöll, E., Ruiz, J., Hövel, P.: Multilayer network analysis of *C. elegans*: Looking into the locomotory circuitry. Neurocomputing **427**, 238–261 (2021)

Appendix A Results for non-induced 4-node motifs in the original network

Table A1: 4-node non-induced motif in *C. elegans* multi-layer network

	Motif	ACh	Electrical	GABA	Glu	MA	Peptides	All	LC
Ind set		180352320	166695375	4249575	60862165	11716640	27646920	247073751	1837620
Only link		35251200	16126750	643500	13391820	1675968	5100720	87422862	1409400
Matching		565812	127869	7707	242243	18938	77172	2557057	87339
Only wedge		4296240	993000	67122	1558790	200320	481452	15727584	564480
Only triangle		276165	42500	1782	72944	3584	19875	1119180	54400
3-star		151148	25391	2418	38490	7598	9484	774463	59533
3-path		250065	24229	2150	88159	5997	19677	1318679	96266
Tailed triangle		75037	6410	443	15060	736	2853	385986	39879
4-cycle		11893	838	51	3632	191	647	57242	6659
Diamond		11136	788	38	1497	51	284	51817	7178
4-clique		728	26	0* [†]	61	2	11	3209	486

NOTE: The values in bold indicate that the discovered motif count is not significant.

* indicates link-swapping random graph generation method

† indicates gnm random graph generation method

Table A2: Percentage of 4-node non-induced motifs in the *C. elegans* multi-layer network relative to ALL

Motif	Motif	ACh	Electrical	GABA	Glu	MA	Peptides
Ind set		73.00	67.47	1.72	24.63	4.74	11.19
Only link		40.32	18.45	0.74	15.32	1.92	5.83
Matching		22.13	5.00	0.30	9.47	0.74	3.02
Only wedge		27.32	6.31	0.43	9.91	1.27	3.06
Only triangle		24.68	3.80	0.16	6.52	0.32	1.78
3-star		19.52	3.28	0.31	4.97	0.98	1.22
3-path		18.96	1.84	0.16	6.69	0.45	1.49
Tailed triangle		19.44	1.66	0.11	3.9	0.19	0.74
4-cycle		20.78	1.46	0.09	6.34	0.33	1.13
Diamond		21.49	1.52	0.07	2.89	0.10	0.55
4-clique		22.69	0.81	0.00	1.9	0.06	0.34

Appendix B Results for non-induced 4-node motifs in the random reference networks

Table B3: Average of 4-node non-induced motifs in the *C. elegans* multi-layer network using link-swapping random graph generation method

	Motif	ACh	Electrical	GABA	Glu	MA	Peptides	All	LC
Ind set		180352320 ±0.00	166695375 ±0.00	4249575 ±0.00	60862165 ±0.00	11716640 ±0.00	27646920 ±0.00	247073751 ±0.00	1837620 ±0.00
		35251200 ±0.00	16126750 ±0.00	643500 ±0.00	13391820 ±0.00	1675968 ±0.00	5100720 ±0.00	8742862 ±0.00	1409400 ±0.00
Only link		571090.02 ±233.64	129108.29 ±105.09	7942.18 ±32.88	244268.16 ±116.50	19560.14 ±56.45	77882.15 ±64.37	2570562.06 ±470.75	89234.01 ±118.40
		2950345.67 ±59576.94	683178.75 ±26272.43	43839.48 ±3255.48	1165909.15 ±22601.23	120686.59 ±7225.18	368538.47 ±10235.52	12000186.61 ±12926.40	412879.12 ±9471.76
Only wedge		55786.86 ±5167.57	6630.75 ±1455.54	542.82 ±237.64	20756.64 ±2276.22	1428.10 ±469.40	5347.33 ±974.25	325675.03 ±12114.61	21905.92 ±16119.39
		57968.20 ±4106.35	8549.89 ±1218.69	806.81 ±184.07	19700.29 ±1090.82	2429.84 ±404.29	5117.26 ±405.77	348002.15 ±14307.91	24723.02 ±1944.71
3-star		120828.99 ±4828.86	13480.70 ±954.50	1294.32 ±186.02	50174.57 ±1963.08	3519.88 ±402.83	12890.50 ±711.18	808285.87 ±16326.50	58105.20 ±2330.79
		9503.82 ±1301.51	6384.43 ±197.70	76.56 ±41.38	3116.37 ±425.14	203.12 ±84.34	636.73 ±137.01	80973.83 ±4902.58	10970.35 ±1243.83
4-cycle		1636.25 ±151.31	9042 ±17.88	11.56 ±4.85	660.71 ±60.88	34.10 ±9.57	133.00 ±18.32	1569.92 ±640.10	2256.32 ±176.21
		378.59 ±105.57	15.05 ±11.25	1.90 ±2.50	99.69 ±29.13	4.71 ±4.19	15.89 ±7.81	3889.99 ±432.92	952.85 ±182.31
4-clique		7.29 ±4.82	0.16 ±0.42	0.02 ±0.14	1.34 ±1.41	0.03 ±0.19	0.16 ±0.41	76.74 ±17.40	30.31 ±10.68

Table B4: Average of 4-node non-induced motifs in the *C. elegans* multi-layer network using gnm random graph generation method

	Motif	ACh	Electrical	GABA	Glu	MA	Peptides	All	LC
Ind set		180352320 ±0.00	166695375 ±0.00	4249575 ±0.00	60862165 ±0.00	11716640 ±0.00	27646920 ±0.00	247073751 ±0.00	1837620 ±0.00
Only link		35251200 ±0.00	16126750 ±0.00	643500 ±0.00	13391820 ±0.00	1675968 ±0.00	5100720 ±0.00	87422862 ±0.00	1409400 ±0.00
Matching		57366221 ±89.64	12976487 ±43.98	805933 ±16.58	245221.81 ±68.17	19882.79 ±23.08	78230.90 ±41.15	2576705.72 ±168.58	89900.10 ±58.82
Only wedge		229443543 ±22859.18	51903175 ±10995.09	32241.83 ±1640.99	98090125 ±13224.56	79387.39 ±2954.83	313086.74 ±6543.56	1030453728 ±46527.26	359591.92 ±4705.35
Only triangle		24740.87 ±2491.19	2779.00 ±827.21	266.90 ±161.03	11962.43 ±1550.42	636.42 ±273.73	3178.89 ±723.04	202457.32 ±7504.90	15230.8 ±1101.68
3-star		24865.06 ±764.47	2778.34 ±183.01	266.77 ±43.41	11960.71 ±492.54	622.66 ±73.81	3194.55 ±210.40	202300.62 ±2769.87	15259.81 ±604.97
3-path		74597.74 ±1498.80	8342.30 ±363.81	801.35 ±84.02	35872.17 ±967.87	1870.06 ±144.04	9584.51 ±408.64	607050.52 ±5479.48	45778.27 ±1178.04
Tailed triangle		2408.34 ±265.23	134.05 ±42.38	19.57 ±13.02	1308.95 ±189.15	44.64 ±21.32	292.01 ±74.46	35757.42 ±1492.20	5803.37 ±524.11
4-cycle		605.81 ±33.94	33.49 ±6.42	5.09 ±2.39	327.86 ±23.72	10.99 ±3.66	73.12 ±10.61	8935.31 ±183.55	1450.8 ±82.48
Diamond		39.05 ±10.21	1.07 ±1.22	0.25 ±0.56	23.91 ±8.64	0.48 ±0.83	4.47 ±3.14	1052.04 ±89.69	366.25 ±63.17
4-clique		0.21 ±0.45	0.00 ±0.04	0.00 ±0.00	0.15 ±0.41	0.00 ±0.03	0.03 ±0.18	10.32 ±3.42	7.70 ±3.48

Appendix C Results for induced 4-node motifs in the original network

Table C5: 4-node induced motif in *C. elegans* multi-layer network

	Motif	ACh	Electrical	GABA	Glu	MA	Peptides	A11	LC
Ind set		149362316	151603860	3675010	49089041	10243629	23059015	175117828	909686
Only link		27262822	14136164	511106	10320884	1285524	4117934	58957465	583181
Matching		394482	110228	6026	173597	13963	61107	1644841	31372
Only wedge		2856576	770279	52337	1126754	158840	368734	9192167	204588
Only triangle		220488	37562	1415	60634	2942	17546	823992	26933
3-star		95471	20453	2051	26180	6956	7155	479275	32066
3-path		110499	12473*	1288*	51761	4043	12955	590133	27108
Tailed triangle		39229	3570	291	9804	556	1849	217226	16999
4-cycle		2941	128	13*	2318	146	396	15052	939
Diamond		6768	632	38	1131	39	218	32563	4262
4-clique		728	26	0*†	61	2	11	3209	486

NOTE: The values in bold indicate that the discovered motif count is not significant.

* indicates link-swapping random graph generation method

† indicates gnm random graph generation method

Appendix D Results for induced 4-node motifs in the random reference networks

Table D6: Average of 4-node induced motifs in the *C. elegans* multi-layer network using link-swapping random graph generation method

	Motif	ACh	Electrical	GABA	Glu	MA	Peptides	All	LC
Ind set		148398740.4 ±48937.91	151352964.65 ±23787.07	3655298.94 ±2826.60	48793569.55 ±18748.68	10173773.45 ±6306.41	22970019.54 ±8817.63	17283256.13 ±96589.37	837903.13 ±5211.09
		28869369.70 ±88678.47	14585318.88 ±45356.39	547525.49 ±5292.90	10828741.94 ±34193.21	1416682.48 ±11824.25	4274943.55 ±16426.30	62359584.30 ±164862.59	671051.85 ±7349.14
Only link		462302.05 ±3888.41	1164117.22 ±919.21	6743.77 ±186.90	198336.03 ±1718.71	16302.25 ±387.14	65863.11 ±673.64	1867082.11 ±12089.58	44797.03 ±1325.12
		22418545.40 ±35651.79	614110.72 ±20417.14	37615.95 ±2319.37	961632.53 ±14366.94	103187.73 ±15161.09	314954.25 ±7249.85	8800017.15 ±56738.75	213399.83 ±1752.16
Only wedge		47011.05 ±4139.10	6021.80 ±1296.22	470.00 ±203.38	17834.27 ±1921.69	1234.26 ±398.85	4741.71 ±855.93	252174.21 ±8434.97	12720.05 ±806.12
		49192.39 ±3381.56	7940.94 ±1139.68	733.99 ±167.96	16777.92 ±887.06	2236.01 ±369.50	4511.65 ±351.11	274501.33 ±11171.21	15537.14 ±1249.31
3-path		97460.37 ±2779.32	11930.59 ±725.25	1106.20 ±136.94	41881.00 ±1333.25	3005.12 ±285.43	11178.37 ±537.60	605993.56 ±8033.02	32492.64 ±654.38
		8076.97 ±950.64	580.11 ±161.09	69.15 ±34.03	2733.74 ±330.61	184.67 ±71.09	575.16 ±113.08	66334.76 ±3441.67	7522.62 ±655.38
4-cycle		1279.54 ±91.48	75.84 ±14.80	9.70 ±4.14	565.05 ±48.52	29.48 ±8.17	117.61 ±16.08	12031.15 ±389.79	1394.39 ±92.55
		334.83 ±82.04	14.11 ±10.24	1.80 ±2.25	91.63 ±23.90	4.52 ±3.92	14.90 ±6.82	3429.55 ±344.29	771.02 ±126.93
4-clique		7.29 ±4.82	0.16 ±0.42	0.02 ±0.14	1.34 ±1.41	0.03 ±0.19	0.16 ±0.41	76.74 ±17.40	30.31 ±10.68

Table D7: Average of 4-node induced motifs in the *C. elegans* multi-layer network using gnm random graph generation method

	Motif	ACh	Electrical	GABA	Glu	MA	Peptides	All	LC
Ind set		147847989.29 ±20017.98	151203688.45 ±10336.32	3645065.54 ±1479.88	48638285.79 ±11392.78	10136868.19 ±2674.92	22921920.4 ±5751.07	171563974.56 ±36841.32	80338.75 ±2749.56
Only link		29875753.09 ±37600.77	14870190.88 ±20116.82	566605.37 ±2831.83	11112531.25 ±21240	1486594.95 ±5120.39	4364520.16 ±10841.47	64522228.72 ±65758.43	711991.01 ±4098.07
Matching		502606.98 ±1435.32	121621.46 ±390.27	7287.23 ±93.82	211266.93±926.73	18078.39 ±155.42	69075.81 ±407.95	2021210.12 ±4711.66	52117.39 ±817.93
Only wedge		2010577.25 ±17088.42	486470.77 ±9709.98	29154.33 ±1342.49	845054.16 ±9569.94	72133.35 ±2412.16	276514.61 ±4978.44	8082398.31 ±28192.74	208545.94 ±1489.13
Only triangle		22409.78 ±2251.02	2647.09 ±788.21	247.84 ±149.64	10700.71 ±1381.60	592.73 ±254.78	2895.68 ±656.18	168762.69 ±6223.75	10129.15 ±716.04
3-star		22533.98 ±681.52	2646.43 ±175.64	247.70 ±40.50	10699.00 ±433.63	578.98 ±68.30	2911.34 ±188.43	168605.99 ±2310.03	10158.16 ±397.68
3-path		67589.56 ±1243.26	7946.66 ±336.59	743.34 ±74.25	32084.52 ±788.98	1739.69 ±125.84	8734.42 ±341.76	505982.83 ±4004.72	30473.47 ±565.05
Tailed triangle		2254.69 ±234.36	129.78 ±39.73	18.57 ±11.69	1215.06 ±162.99	42.73 ±19.62	274.53 ±66.38	31673.12 ±1182.17	4430.73 ±314.52
4-cycle		567.40 ±32.38	32.42 ±6.30	4.84 ±2.32	304.39 ±22.03	10.51 ±3.61	68.75 ±10.08	7914.24 ±163.60	1107.64 ±62.96
Diamond		37.77 ±9.63	1.06 ±1.19	0.25 ±0.56	23.04 ±7.95	0.47 ±0.79	4.27 ±2.85	990.11 ±79.34	320.07 ±48.76
4-clique		0.21 ±0.45	0.00 ±0.04	0.00 ±0.00	0.15 ±0.41	0.00 ±0.03	0.03 ±0.18	10.32 ±3.42	7.70 ±3.48

Appendix E Results for non-induced 5-node motifs in the original network

Table E8: 5-node non-induced motifs in the *C. elegans* multi-layer network

	Motif	ACh	Electrical	GABA	Glu	MA	Peptides	All	LC
Ind set		9161897856	8301429675	83291670	2349279569	297602656	873642672	13589056305	29034396
Only link		2984601600	1338520250	21021000	861540420	70949312	268637920	8013762350	37114200
Matching		143716248	31839381	755286	46752899	2405126	12193176	703190675	6899781
wedge+link		17205321	1908523	75176	5379794	279633	1139991	125235528	2682077
Traingle+link		1091354	80460	1843	250020	4864	46897	8875634	253881
4-star		1405355	179490	7573	154375	32288	24010	11375923	483097
Prong		6398697	366720	19903	1233301	71213	168770	49972614	2135837
4-path		3881202	171761	7042	986172	32579	132148	31321978	1325556
Forktailed-tri		1262834	78343	2568	114927	5679	12009	9593669	566754
Lontailed-tri		1079519	30415	859	165198	1884	18624	8506399	480460
Doubletailed-tri		1777988	73070	2788	202772	6143	20643	12624398	745673

Table E8: 5-node non-induced motifs in the *C. elegans* multi-layer network

Tailed-4-cycle		1148058	47031	1240	195598	6411	19712	8027537	532415
5-cycle		120769	2419	49*	20889	338	2256	911648	61511
Hounglass		94495	2194	28	7649	58	725	708143	54653
Cobra		472031	9902	199	39076	218	3759	3067571	228874
Stingray		721513	36472	812	43572	1167	4327	4724609	375170
Hatted-4-cycle		292288	5064	69	29689	276	2779	1906636	160352
3-wedge-col		66701	3590	68	9044	267	747	399286	38039
3-tri-collison		51458	3441	58	1823	39	219	306445	32511
Tailed-4-clique		85830	1501	0*	3335	23	295	507147	43685
Triangle-strip		168237	2765	18	7440	41	681	999638	97719
Diamond-wed-col		65355	740	8	4492	26	356	361078	36360
4-Wheel		16763	83	1	570	3	30	83562	9391

Table E8: 5-node non-induced motifs in the *C. elegans* multi-layer network

Hatted-4-clique		44524	540	0^{*†}	974	10	84	236759	26204
Almost-5-clique		6929	20	0^{*†}	82	1	2	32569	3868
5-clique		386	0^{*†}	0^{*†}	1	0^{*†}	0^{*†}	1670	193

NOTE: The values in bold indicate that the discovered motif count is not significant.

* indicates link-swapping random graph generation method

† indicates gnm random graph generation method

Appendix F Results for non-induced 5-node motifs in the random reference networks

Table F9: Average of 5-node non-induced motif in *C. elegans* multi-layer network using link-swapping random graph generation method

	Motif	ACh	Electrical	GABA	Glu	MA	Peptides	All	LC
Ind set		9161897856	8301429675	83291670	2349279569	297602656	873642672	13589056305	29034396
		± 0.00	± 0.00	± 0.00	± 0.00	± 0.00	± 0.00	± 0.00	± 0.00
Only link		2984601600	1338320250	21021000	861540420	70949312	268637920	8013762350	37114200
		± 0.00	± 0.00	± 0.00	± 0.00	± 0.00	± 0.00	± 0.00	± 0.00
Matching		145056864.32	32147962.97	778333.35	47143754.69	24841137.27	12305379.38	703904567.33	7049486.87
		± 59343.31	± 26167.34	± 3222.59	± 22484.73	± 7168.73	± 10171.15	± 12945.66	± 9353.36
wedge+link		12056222.76	1346459.44	51655.83	4083776.75	175152.91	883589.27	96685252.89	2043507.33
		± 231072.67	± 48631.08	± 3364.07	± 75292.68	± 9507.48	± 23152.13	± 1003103.60	± 41058.72
Triangle+link		226113.62	12914.83	619.78	72313.69	2028.28	12748.41	2614105.05	107321.62
		± 20613.83	± 2798.90	± 267.07	± 7868.82	± 656.43	± 2307.97	± 95735.62	± 7574.21
4-star		301106.87	33079.52	1484.22	53861.05	6173.14	9272.43	2768053.59	109192
		± 46498.56	± 9116.55	± 626.73	± 5850.24	± 1848.78	± 1467.69	± 265697.79	± 18122.95
Prong		1760219.93	113109.56	6235.86	485613.14	23162.02	82459.19	18841230.95	787686.15
		± 155356.56	± 18421.72	± 1796.77	± 36040.32	± 5091.33	± 8623.10	± 897712.1	± 69551.88
4-path		1256407.62	66762.97	3725.12	416025.01	13623.97	71207.59	14955798.09	642239.82
		± 75951.64	± 70911.59	± 783.62	± 24649.83	± 2246.02	± 5869.56	± 444045.61	± 36449.22
Forktailed-tri		94637.01	4439.74	260.7	16807.84	931.53	2201.95	1220332.84	90733.93
		± 19908.02	± 1976.44	± 178.46	± 3030.36	± 498.16	± 606.88	± 132808.83	± 17032.67
Lontailed-tri		96324.79	2824.19	189.65	25650.21	654.01	3439.81	1463389.81	116302.76
		± 15433.57	± 927.22	± 112.93	± 3987.42	± 303.60	± 812.89	± 101243.85	± 14645.97
Doubletailed-tri		134849.47	4584.01	310.59	29919.87	1093.84	3913.59	1802883.01	138182.49
		± 26559.39	± 2156.15	± 224.46	± 5222.24	± 620.48	± 1029.82	± 161417.33	± 21515.90

Table F9: Average of 5-node non-induced motif in *C. elegans* multi-layer network using link-swapping random graph generation method

		94376.22	2920.34	199.95	25477.97	809.83	3330.35	1436307.44	118105.54
Tailed-4-cycle		±13509.84	±835.51	±108.70	±3251.30	±300.99	±599.83	±961.52.48	±14268.97
5-cycle		13146.44	322.61	24.13	4231.93	94.91	566.20	228900.30	19606.57
Hourglass		2481.25	47.43	3.31	441.65	11.28	44.57	45064.33	6288.93
Cobra		10476.32	175.32	12.48	1915.22	40.53	191.14	169096.06	23100.66
Stingray		14745.66	399.48	23.57	2135.34	78.60	210.99	224529.11	29565.64
Hatted-4-cycle		7186.27	105.49	8.48	1572.43	32.27	157.39	135311.30	20076.45
3-wedge-col		1259.95	28.54	1.73	273.71	7.82	26.58	22963.38	3489.66
3-tri-collision		277.13	7.32	0.31	26.26	0.91	1.97	4566.32	989.83
Tailed-4-clique		±164.60	±14.56	±1.11	±17.19	±2.18	±2.44	±1237.44	±381.89
Triangle-strip		544.64	6.28	0.34	57.70	0.80	4.16	8403.58	1757.76
Diamond-wed-col		408.99	3.36	0.26	61.97	0.93	4.59	7753.63	1915.81
		±205.74	±4.27	±0.90	±30.54	±1.82	±3.94	±1463.12	±559.37

Table F9: Average of 5-node non-induced motif in *C. elegans* multi-layer network using link-swapping random graph generation method

4-Wheel		31.73 ±28.81	0.13 ±0.55	0.01 ±0.14	2.90 ±3.47	0.03 ±0.21	0.14 ±0.44
Hatted-4-clique		87.04 ±90.16	0.57 ±2.12	0.03 ±0.33	6.59 ±10.31	0.05 ±0.42	0.35 ±1.13
Almost-5-clique		4.50 ±8.17	0.01 ±0.13	0.00 ±0.03	0.23 ±0.90	0.00 ±0.00	0.00 ±0.06
5-clique		0.10 ±0.41	0.00 ±0.00	0.00 ±0.00	0.00 ±0.05	0.00 ±0.00	0.00 ±1.54
						1.15 0.72	0.72 ±1.22
						555.67 ±184.19	207.22 ±97.78
						1451.08 ±570.85	495.47 ±267.53

Table F10: Average of 5-node non-induced motif in *C. elegans* multi-layer network using gnm random graph generation method

	Motif	ACh	Electrical	GABA	Glu	MA	Peptides	All	LC
Ind set		9161897856 ±0.00	8301429675 ±0.00	83291670 ±0.00	2349279569 ±0.00	297602656 ±0.00	873642672 ±0.00	13589056305 ±0.00	29034396 ±0.00
		2984601600 ±0.00	1338520250 ±0.00	21021000 ±0.00	861540420 ±0.00	70949312 ±0.00	268637920 ±0.00	8013762350 ±0.00	37114200 ±0.00
Only link		145710202.36 ±22769.54	32311453.38 ±10951.11	789813.85 ±1624.41	47327808.94 ±13156.39	2525113.82 ±2931.74	12360482.36 ±6502.41	708594073 ±46358.68	7102107.98 ±4646.53
		9475531.58 ±91427.32	1037324.06 ±21282.06	39275.31 ±1839.89	3461860.08 ±44767.78	119039.99 ±4154.95	756857.87 ±15010.87	83487911.29 ±366089.38	1808384.13 ±21324.8
Matching		102085.44 ±10265.62	5546.23 ±1650.46	322.82 ±194.53	42162.76 ±5452.00	949.76 ±407.88	7665.21 ±1738.95	1639650.23 ±6660.05	76442.95 ±5446.38
		51277.76 ±3356.75	2772.37 ±403.34	160.14 ±62.21	21085.27 ±1837.90	463.33 ±129.39	3848.88 ±565.75	818595.54 ±23125.48	38288.61 ±3138.37
wedge+link		615473.90 ±18626.54	33325.20 ±2224.89	1936.27 ±310.22	252857.96 ±10245.80	5569.91 ±883.96	46229.76 ±4052.25	9827894.43 ±178358.34	459452.01 ±23694.60
		9917.03 ±1323.84	267.62 ±100.21	23.12 ±20.43	4603.84 ±825.72	66.22 ±40.93	46234.96 ±2978.57	9830537.29 ±132926.08	459497.04 ±17387.90
4-path		19849.53 ±2283.71	535.8 ±175.47	46.83 ±32.98	9216.53 ±1409.61	132.53 ±67.04	46229.76 ±227.38	9827894.43 ±15027.1	459452.01 ±3630.40
		19827.12 ±2495.8	535.85 ±196.01	46.81 ±38.66	9205.79 ±1553.78	132.06 ±77.27	1402.72 ±372.99	578776.7 ±25733.03	29049.18 ±5776.44
Forktailed-tri		19827.12 ±2495.8	535.85 ±196.01	46.81 ±38.66	9205.79 ±1553.78	132.06 ±77.27	1409.44 ±428.25	578635.28 ±28050.75	58108.52 ±6529.90
Lontailed-tri									
Doubletailed-tri									

Table F10: Average of 5-node non-induced motif in *C. elegans* multi-layer network using gram random graph generation method

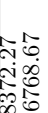
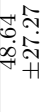
Tailed-4-cycle		19971.53 ±1470.95	533.79 ±118.71	48.64 ±27.27	9233.40 ±884.86	129.83 ±52.02	1403.36 ±252.10	578372.27 ±16768.67	58131.02 ±4723.06
5-cycle		3993.27 ±215.91	107.23 ±16.60	9.36 ±4.18	1844.03 ±133.12	25.58 ±7.30	281.22 ±34.47	115702.60 ±2660.32	11654.32 ±755.20
Hourglass		159.78 ±38.42	2.16 ±2.07	0.27 ±0.66	83.86 ±27.49	0.80 ±1.18	10.56 ±6.83	8516.31 ±737.66	1833.40 ±338.19
Cobra		642.71 ±178.78	8.60 ±10.56	1.19 ±3.01	336.27 ±130.98	2.84 ±5.34	42.88 ±33.15	34026.44 ±3107.27	7321.16 ±1407.80
Stingray		642.22 ±185.27	8.46 ±10.61	1.18 ±2.88	336.74 ±138.12	2.80 ±5.42	43.27 ±34.96	34018.77 ±3243.51	7314.75 ±1501.01
Hatted-4-cycle		642.84 ±97.48	8.61 ±4.92	1.16 ±1.66	336.03 ±68.05	2.89 ±2.58	41.99 ±15.92	34034.34 ±1925.82	7340.42 ±1011.43
3-wedge-col		107.79 ±19.55	1.42 ±1.39	0.17 ±0.45	56.17 ±13.09	0.48 ±0.82	7.06 ±3.83	5666.54 ±295.45	1221.05 ±167.99
3-tri-collision		3.47 ±2.85	0.02 ±0.13	0.00 ±0.03	2.07 ±2.31	0.01 ±0.15	0.23 ±0.60	333.15 ±57.46	152.86 ±51.00
Tailed-4-clique		7.01 ±14.95	0.04 ±0.81	0.00 ±0.00	4.09 ±12.11	0.01 ±0.22	0.64 ±3.67	667.24 ±226.66	306.9 ±146.56
Triangle-strip		20.81 ±11.29	0.14 ±0.49	0.03 ±0.18	12.38 ±9.23	0.06 ±0.30	1.28 ±2.21	2001.56 ±292.29	919.73 ±271.41
Diamond-wed-col		10.44 ±4.88	0.07 ±0.29	0.01 ±0.12	6.17 ±3.96	0.03 ±0.19	0.58 ±0.94	969.91 ±111.44	460.89 ±111.01

Table F10: Average of 5-node non-induced motif in *C. elegans* multi-layer network using gnm random graph generation method

		0.17 ±0.44	0.00 ±0.00	0.00 ±0.00	0.12 ±0.43	0.00 ±0.00	0.01 ±0.08	29.39 ±8.77	28.72 ±13.88
4-Wheel									
Hatted-4-clique		0.34 ±1.09	0.00 ±0.00	0.00 ±0.00	0.22 ±0.98	0.00 ±0.03	0.03 ±0.26	59.15 ±25.08	57.64 ±36.04
Almost-5-clique		0.01 ±0.07	0.00 ±0.00	0.00 ±0.00	0.00 ±0.07	0.00 ±0.00	0.00 ±0.00	1.12 ±1.53	2.41 ±3.29
5-clique		0.00 ±0.00	0.00 ±0.00	0.00 ±0.00	0.00 ±0.00	0.00 ±0.00	0.00 ±0.08	0.01 ±0.08	0.03 ±0.19

Appendix G Results for induced 5-node motifs in the original network

Table G11: 5-node induced motifs in the *C. elegans* multi-layer network

	Motif	ACh	Electrical	GABA	Glu	MA	Peptides	All	LC
Ind set		6740603526	7101053698	65779414	1653421431	239778812	648734427	7765614959	9616064
Only link		1961317251	1077646814	14473518	557053610	46487282	186951607	4165138807	9254750
Matching		81968440	24630869	489193	27068856	1412560	8050245	334089336	1357434
wedge+link		7760852	1281903	47297	278974*	167551	715979	48067402	390866
Traingle+link		575040	62720	1260	146406	3469	34252	4396960	55008
4-star		688500	129768	5712	78525	27712	15831	5563054	190900
Prong		1658015	133846	10568	476066	41387	87142	13208481	305438
4-path		55959	53350*	2618*	353578	14198	61360	6627552	107706
Forktailed-tri		370878	30103	1286	46876	3578	5385	3297305	131420
Lontailed-tri		214157	10032	351	60261	997	8327	2109920	58681
Doubletailed-tri		385163	13739	1155	75827	3632	8129	3016956	93356

Table G11: 5-node induced motifs in the *C. elegans* multi-layer network

Tailed-4-cycle		113972	3910	151*	67539	3409	7929	972426	27066[†]
5-cycle		8270	308*	10*[†]	3876	129	594	94414	2518
Hourglass		13048	555	12	2820	37	260	178783	7811
Cobra		94517	2893	155	15651	95*	1664	705810	33169
Stingray		187957	11045	432	17861	870	1678	1385604	71963
Hatted-4-cycle		19558	330	13*	7617	162	809	204890	8138*
3-wedge-col		4082	35*	4*	4525	214	308	22070	612[†]
3-tri-collision		23861	2961	58	1085	32	141	150693	15981
Tailed-4-clique		30636	541	0*[†]	1859	9*	139	195643	10625
Triangle-strip		24651	633	14	2680	7*	261	204396	13383
Diamond-wed-col		4560	48	4	1946	13	170	33092	1614
4-Wheel		1766	23	1	339	0*[†]	24	10905	682

Table G11: 5-node induced motifs in the *C. elegans* multi-layer network

Hatted-4-clique		14530	420	0^{*†}	512	4	72	91445	8786
Almost-5-clique		3069	20	0^{*†}	72	1	2	15869	1938
5-clique		386	0^{*†}	0^{*†}	1	0^{*†}	0^{*†}	1670	193

NOTE: The values in bold indicate that the discovered motif count is not significant.

* indicates link-swapping random graph generation method

† indicates grm random graph generation method

Table G12: Ratio of 5-node induced vs non-induced motifs in the *C. elegans* multi-layer network

	Motif	ACh	Electrical	GABA	Glu	MA	Peptides	All	LC
Ind set		0.74	0.86	0.79	0.70	0.81	0.74	0.57	0.33
Only link		0.66	0.81	0.69	0.65	0.66	0.70	0.52	0.25
Matching		0.57	0.77	0.65	0.58	0.59	0.66	0.48	0.2
wedge+link		0.45	0.67	0.63	0.52	0.6	0.63	0.38	0.15
Triangle+link		0.53	0.78	0.68	0.59	0.71	0.73	0.50	0.22
4-star		0.49	0.72	0.75	0.51	0.86	0.66	0.49	0.40
Prong		0.26	0.36	0.53	0.39	0.58	0.52	0.26	0.14
4-path		0.19	0.31	0.37	0.36	0.44	0.46	0.21	0.08
Forktailed-tri		0.29	0.38	0.50	0.41	0.63	0.45	0.34	0.23
Lontailed-tri		0.20	0.33	0.41	0.36	0.53	0.45	0.25	0.12
Doubletailed-tri		0.22	0.19	0.41	0.37	0.59	0.39	0.24	0.13

Table G12: Ratio of 5-node induced vs non-induced motifs in the *C. elegans* multi-layer network

Tailed-4-cycle		0.10	0.08	0.12	0.35	0.53	0.40	0.12	0.05
5-cycle		0.07	0.13	0.20	0.19	0.38	0.26	0.10	0.04
Hourglass		0.14	0.25	0.43	0.37	0.64	0.36	0.25	0.14
Cobra		0.2	0.29	0.78	0.40	0.44	0.44	0.23	0.14
Stingray		0.26	0.3	0.53	0.41	0.75	0.39	0.29	0.19
Hatted-4-cycle		0.07	0.07	0.19	0.26	0.59	0.29	0.11	0.05
3-wedge-col		0.06	0.01	0.06	0.5	0.8	0.41	0.06	0.02
3-tri-collison		0.46	0.86	1.00	0.60	0.82	0.64	0.49	0.49
Tailed-4-clique		0.36	0.36	-	0.56	0.39	0.47	0.39	0.24
Triangle-strip		0.15	0.23	0.78	0.36	0.17	0.38	0.2	0.14
Diamond-wed-col		0.07	0.06	0.50	0.43	0.5	0.48	0.09	0.04
4Wheel		0.11	0.28	1.00	0.59	0.00	0.80	0.13	0.07

Table G12: Ratio of 5-node induced vs non-induced motifs in the *C. elegans* multi-layer network

		0.33	0.78	1.00	0.53	0.40	0.86	0.39	0.34
Almost-5-clique		0.44	1.00	-	0.88	1.00	1.00	0.49	0.50
5-clique		1.00	-	-	1.00	-	-	1.00	1.00

Table G13: Percentage of 5-node non-induced motifs in the *C. elegans* multi-layer network relative to ALL

Motif	ACh	Electrical	GABA	Glu	MA	Peptides
Ind set		67.42	61.09	0.61	17.29	2.19
Only link		37.24	16.70	0.26	10.75	0.89
Matching		20.44	4.53	0.11	6.65	0.34
wedge+link		13.74	1.52	0.06	4.30	0.22
Triangle+link		12.30	0.91	0.02	2.82	0.05
4-star		12.35	1.58	0.07	1.36	0.28
Prong		12.80	0.73	0.04	2.47	0.14
4-path		12.39	0.55	0.02	3.15	0.10
Forktailed-tri		13.16	0.82	0.03	1.20	0.06
Lontailed-tri		12.69	0.36	0.01	1.94	0.02
Doubtetailed-tri		14.08	0.58	0.02	1.61	0.05
						0.16

Table G13: Percentage of 5-node non-induced motifs in the *C. elegans* multi-layer network relative to ALL

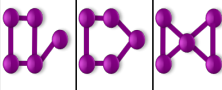
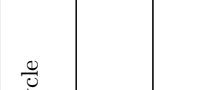
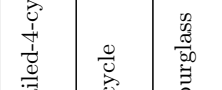
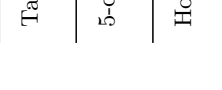
Tailed-4-cycle		14.30	0.59	0.02	2.44	0.08	0.25
5-cycle		13.25	0.27	0.01	2.29	0.04	0.25
Hourglass		13.34	0.31	0.00	1.08	0.01	0.10
Cobra		15.39	0.32	0.01	1.27	0.01	0.12
Stingray		15.27	0.77	0.02	0.92	0.02	0.09
Hatted-4-cycle		15.33	0.27	0.00	1.56	0.01	0.15
3-wedge-col		16.71	0.90	0.02	2.27	0.07	0.19
3-tri-collision		16.79	1.12	0.02	0.59	0.01	0.07
Tailed-4-clique		16.92	0.30	0.00	0.66	0.00	0.06
Triangle-strip		16.83	0.28	0.00	0.74	0.00	0.07
Diamond-wed-col		18.10	0.20	0.00	1.24	0.01	0.10
4-Wheel		20.06	0.10	0.00	0.68	0.00	0.04

Table G13: Percentage of 5-node non-induced motifs in the *C. elegans* multi-layer network relative to ALL

		18.81	0.23	0.00	0.41	0.00	0.04
Hatted-4-clique		18.81	0.23	0.00	0.41	0.00	0.04
Almost-5-clique		21.27	0.06	0.00	0.25	0.00	0.01
5-clique		23.11	0.00	0.00	0.06	0.00	0.00

Appendix H Results for induced 5-node motifs in the random reference networks

Table H14: Average of 5-node induced motifs in the *C. elegans* multi-layer network using link-swapping random graph generation method

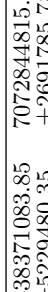
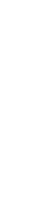
	Motif	ACh	Electrical	GABA	Glu	MA	Peptides	All	LC
Ind set		6638371083.85 ±5229480.35	7072844815.9 ±2691785.78	64932551.47 ±120832.81	1629462881.71 ±1525880.11	235850729.88 ±351790.57	642555395.89 ±604903.08	7531898979.22 ±9971651.86	8035600.37 ±114950.68
Only link		2115708236.85 ±8629544.32	1125545846.85 ±4890598.66	15943319.11 ±211424.78	594490370.04 ±2534900.87	53437636.13 ±618288.58	197138635.66 ±1046443.55	4447858263.12 ±14257168.69	1033045.58 ±99746.4
Matching		100017439.93 ±1047257.75	26716330.47 ±273614.95	580175.54 ±19798.00	32229221.98 ±361024.55	1802666.56 ±53233.94	9012909.30 ±121488.06	392532167.53 ±3198412.76	199271.10 ±66893.27
wedge +link		8051848.84 ±69827.44	1093303.71 ±26037.61	38261.59 ±1615.41	2796428.48 ±21885.89	126558.81 ±4545.63	6341133.57 ±8796.75	5366681.869 ±265746.32	600960.88 ±19499.07
Triangle +link		149192.44 ±11679.31	10432.00 ±2169.41	455.50 ±193.36	50607.89 ±5194.90	1462.57 ±454.91	9714.46 ±1709.10	1487234.60 ±44341.91	34007.58 ±2419.85
4-star		221680.24 ±34552.80	29055.27 ±8140.29	1248.76 ±538.94	39397.92 ±4247.40	5326.67 ±1607.10	7308.74 ±1170.24	1782894.93 ±177780.68	47027.00 ±8611.91
Prong		1156830.80 ±75903.16	89597.09 ±12700.75	4712.99 ±1210.39	340940.65 ±20760.49	17564.76 ±3279.17	62716.83 ±5783.52	10745479.93 ±365075.66	263514.84 ±13608.48
4-path		794020.37 ±26731.77	51443.45 ±4207.49	2680.49 ±428.57	286470.67 ±11876.15	9720.22 ±1153.87	53356.91 ±3475.44	8248965.73 ±117470.96	198303.27 ±5846.76
Forktailed- tri		66052.51 ±11558.34	3638.95 ±1361.61	21179 ±128.35	12335.98 ±1813.85	766.09 ±362.49	1741.92 ±414.34	781329.24 ±74126.36	39869.65 ±6264.29
Lontailed- tri		60402.07 ±6411.55	2173.67 ±568.71	141 ±67.56	18159.26 ±2199.29	484.18 ±182.37	2658.37 ±531.72	842558.45 ±35954.10	41149.65 ±2117.00

Table H14: Average of 5-node induced motifs in the *C. elegans* multi-layer network using link-swapping random graph generation method

Doubledetailed-tri		87867.79 ±12821.39	3473.41 ±1317.44	238.74 ±146.90	21564.99 ±2999.27	847.84 ±41.66	3050.80 ±688.72	1064837.67 ±67829.72
Tailed-4-cycle		56809.34 ±5518.77	2091.28 ±535.28	144.01 ±73.06	17897.89 ±1923.37	602.73 ±201.41	2548.79 ±421.43	805132.64 ±37359.72
5-cycle		7613.42 ±507.89	233.98 ±41.32	16.81 ±6.97	2897.47 ±247.84	66.60 ±18.35	426.79 ±58.11	124504.51 ±3676.76
Hourglass		1582.81 ±365.10	37.03 ±22.69	2.65 ±3.16	321.83 ±79.85	9.10 ±7.98	35.50 ±15.56	28548.19 ±3033.45
Cobra		6651.58 ±1695.95	131.64 ±89.57	9.76 ±13.28	1413.78 ±382.71	32.26 ±31.79	153.21 ±71.57	102606.15 ±10415.27
Stingray		10123.29 ±2958.17	319.24 ±287.75	19.51 ±25.59	1601.83 ±444.54	66.72 ±64.70	170.56 ±81.64	146828.00 ±19845.37
Hatted-4-cycle		4130.30 ±656.61	73.32 ±28.86	6.26 ±5.21	1118.58 ±196.28	24.58 ±15.02	122.63 ±34.27	77845.4 ±5284.27
3-wedge-col		707.31 ±155.37	18.66 ±17.46	1.20 ±1.89	196.96 ±46.36	6.10 ±5.16	20.63 ±8.87	12950.30 ±1176.47
3-tri-collison		202.61 ±106.78	6.78 ±13.94	0.29 ±1.07	20.35 ±11.33	0.86 ±2.09	1.64 ±2.01	3304.02 ±822.07
Tailed-4-clique		395.60 ±274.55	5.20 ±14.71	0.29 ±2.41	45.87 ±48.57	0.70 ±4.38	3.50 ±8.89	5878.97 ±1465.53
Triangle-strip		710.51 ±287.91	9.11 ±11.03	0.59 ±1.47	103.51 ±45.94	2.01 ±3.34	8.16 ±6.93	13251.97 ±2315.85

Table H14: Average of 5-node induced motifs in the *C. elegans* multi-layer network using link-swapping random graph generation method

		232.60	2.36	0.19	45.79	0.75	3.73	4646.19	865.20
Diamond-wed-col		232.60 ±74.49	2.36 ±2.51	0.19 ±0.59	45.79 ±16.94	0.75 ±1.32	3.73 ±2.78	4646.19 ±569.31	865.20 ±148.16
4-Wheel		19.69 ±12.48	0.10 ±0.40	0.01 ±0.10	2.25 ±2.29	0.03 ±0.21	0.13 ±0.37	372.66 ±91.97	119.56 ±41.46
Hatted-4-clique		62.96 ±53.53	0.51 ±1.69	0.02 ±0.22	5.28 ±6.82	0.05 ±0.42	0.32 ±0.97	1085.06 ±365.50	320.15 ±141.48
Almost-5-clique		3.53 ±5.19	0.01 ±0.13	0.00 ±0.03	0.20 ±0.64	0.00 ±0.00	0.00 ±0.06	55.24 ±30.17	25.63 ±17.73
5-clique		0.10 ±0.41	0.00 ±0.00	0.00 ±0.00	0.00 ±0.05	0.00 ±0.00	0.00 ±1.54	1.15 ±1.54	0.72 ±1.22

Table H15: Average of 5-node induced motifs in the *C. elegans* multi-layer network using gnm random graph generation method

Motif	ACh	Electrical	GABA	Glu	MA	Peptides	All	LC
Ind set		6578587162.18 ±2218300.93	7055801840.73 ±1201243.91	64489879.45 ±64937.65	1616723295.44 ±943091.19	233762601.6 ±153206.55	639227916.13 ±398518.73	738086.6 ±62411.58
Only link		2215842909.09 ±3869772.26	1156661639.74 ±2259752.04	16726650.94 ±117753.49	615761847.79 ±1616945	57169207.7 ±278645.58	202972466.95 ±701227.58	10849646.9 ±58400.44
Matching		111846848.16 ±448172.92	28384329.33 ±127044.13	645648.57 ±11163.6	35127451.28 ±214967.79	2086901.45 ±24398.46	9636868.56 ±78450	435961597.06 ±1405103.04
wedge+		7520875.51 ±39137.84	926791.41 ±14845.66	32976.59 ±105.02	2667882.72 ±17456.78	100817.06 ±2389.44	609192.44 ±6937.41	2385766.75 ±46589.13
link		83773.15 ±8387.30	5031.49 ±1498.74	278.79 ±168.74	33746.16 ±4322.97	824.37 ±353.89	6364.24 ±1435.80	54593519.96 ±82503.95
Traingle+		42128.79 ±2731.88	2515.16 ±370.33	138.44 ±54.07	16881.96 ±1459.24	400.62 ±113.49	3195.78 ±465.62	697764.59 ±10994.98
4-star		505365.82 ±18901.37	30231.17 ±2610.39	1667.67 ±346.74	202404.97 ±10060.57	4815.31 ±715.85	38405.16 ±3082.33	1139585.12 ±41860.29
Prong		505272.07 ±12998.57	30240.02 ±1886.57	1668.56 ±239.98	202334.90 ±6886.17	4827.29 ±506.33	6828721.93 ±109047.13	203860.10 ±7397.02
4-path		8414.02 ±1001.20	247.02 ±86.83	20.31 ±16.30	3822.28 ±590.00	59.29 ±33.75	38418.52 ±2124.19	6831252.69 ±70495.45
Forktailed-tri		16841.26 ±1752.86	494.14 ±152.80	41.31 ±26.50	7655.63 ±1034.12	118.44 ±55.56	1203.31 ±289.18	213608.69 ±8981.44
Lontailed-tri		16816.51 ±1905.37	494.42 ±170.98	41.11 ±31.08	7642.87 ±1126.36	118.43 ±64.95	1208.49 ±332.80	427453.60 ±15661.46
Doubletailed-tri								29601.01 ±1834.75

Table H15: Average of 5-node induced motifs in the *C. elegans* multi-layer network using gnm random graph generation method

Tailed-4-cycle		16956.21 ±1196.69	492.37 ±108.03	4315 ±23.55	7670.42 ±695.25	116.14 ±46.09	1203.39 ±206.78	427118.49 ±11531.43	29610.88 ±205.83
5-cycle		3390.80 ±170.12	98.91 ±15.34	8.26 ±3.72	1531.83 ±104.57	22.81 ±6.59	241.57 ±28.97	85440.42 ±1740.06	5939.3 ±305.44
Hourglass		139.95 ±32.19	2.02 ±1.93	0.24 ±0.62	72.14 ±22.27	0.75 ±1.11	9.36 ±5.89	6685.20 ±519.42	1072.47 ±15.40
Cobra		563.12 ±146.07	8.07 ±9.56	1.11 ±2.73	289.54 ±101.77	2.64 ±4.83	37.57 ±26.19	26703.56 ±2130.87	4274.40 ±621.83
Stingray		562.69 ±147.36	7.97 ±9.46	1.12 ±2.65	289.91 ±103.92	2.60 ±4.72	37.81 ±26.97	26697.51 ±2170.22	4273.05 ±652.33
Hatted-4-cycle		563.39 ±75.18	8.03 ±4.38	1.05 ±1.43	289.27 ±49.10	2.65 ±2.28	37.4 ±12.86	26712.63 ±1188.73	4292.15 ±385.82
3-wedge-col		94.53 ±17.85	1.33 ±1.35	0.16 ±0.42	48.38 ±11.49	0.43 ±0.77	6.30 ±3.53	4446.98 ±237.16	713.09 ±101.60
3-tri-collison		315 ±2.56	0.02 ±0.13	0.00 ±0.03	1.86 ±2.10	0.01 ±0.15	0.19 ±0.54	277.31 ±43.88	102.09 ±29.15
Tailed-4-clique		6.36 ±13.47	0.04 ±0.81	0.00 ±0.00	3.67 ±10.68	0.01 ±0.16	0.57 ±3.28	555.56 ±185.32	205.36 ±91.57
Triangle-strip		18.86 ±9.29	0.14 ±0.49	0.03 ±0.18	11.07 ±7.38	0.05 ±0.28	1.12 ±1.72	1667.24 ±215.09	615.55 ±143.84
Diamond-wed-col		9.47 ±4.13	0.07 ±0.29	0.01 ±0.12	5.50 ±3.12	0.03 ±0.18	0.52 ±0.81	833.12 ±77.47	309.01 ±53.82

Table H15: Average of 5-node induced motifs in the *C. elegans* multi-layer network using gnm random graph generation method

		0.00 ±0.00	0.00 ±0.00	0.11 ±0.37	0.00 ±0.00	0.01 ±0.08	26.11 ±7.16	22.01 ±9.20
4-Wheel		0.15 ±0.40	0.00 ±0.00	0.00 ±0.00	0.00 ±0.00	0.00 ±0.08	26.11 ±7.16	22.01 ±9.20
Hatted-4-clique		0.31 ±0.90	0.00 ±0.00	0.00 ±0.00	0.21 ±0.77	0.00 ±0.03	0.03 ±0.26	52.58 ±20.14
Almost-5-clique		0.01 ±0.07	0.00 ±0.00	0.00 ±0.00	0.00 ±0.07	0.00 ±0.00	0.00 ±0.00	1.07 ±1.23
5-clique		0.00 ±0.00	0.00 ±0.00	0.00 ±0.00	0.00 ±0.00	0.00 ±0.00	0.01 ±0.08	0.03 ±0.19